BBA - Biomembranes 1863 (2021) 183569

Contents lists available at ScienceDirect

BBA - Biomembranes

journal homepage: www.elsevier.com/locate/bbamem

Membrane properties of amacrocyclic tetraether bisphosphatidylcholine lipid: Effect of a single membrane-spanning polymethylene cross-linkage between two head groups of ditetradecylphosphatidylcholine membrane

Naoyuki Tsuchida [a], Toshiyuki Takagi [b,*], Hiroshi Takahashi [c,*], Toshitada Yoshihara [a], Seiji Tobita [a], Masashi Sonoyama [a,d,e,**]

[a] Division of Molecular Science, Faculty of Science and Technology, Gunma University, Kiryu, Gunma 376-8515, Japan
[b] Cellular and Molecular Biotechnology Research Institute, AIST, Tsukuba, Ibaraki 305-8565, Japan
[c] Division of Pure and Applied Science, Faculty of Science and Technology, Gunma University, Maebashi, Gunma 371-8510, Japan
[d] Gunma University Initiative for Advanced Research (GIAR), Gunma University, Kiryu, Gunma 376-8515, Japan
[e] Gunma University Center for Food Science and Wellness (GUCFW), Gunma University, Kiryu, Gunma 376-8515, Japan

ARTICLE INFO

Keywords:
Amacrocyclic phospholipid
Ether-linked phospholipid
Thermotropic transition
Membrane fluidity
Leakage assay

ABSTRACT

The plasma membranes of archaea are abundant in macrocyclic tetraether lipids that contain a single or double long transmembrane hydrocarbon chains connecting the two glycerol backbones at both ends. In this study, a novel amacrocyclic bisphosphatidylcholine lipid bearing a single membrane-spanning octacosamethylene chain, 1,1'-*O*-octacosamethylene-2,2′-di-*O*-tetradecyl-bis-(*sn*-glycero)-3,3′-diphosphocholine (AC-(di-*O*-C14PC)$_2$), was synthesized to elucidate effects of the interlayer cross-linkage on membrane properties based on comparison with its corresponding diether phosphatidylcholine, 1,2-di-*O*-tetradecyl-*sn*-glycero-3-phosphocholine (DTPC), that forms bilayer membrane. Several physicochemical techniques demonstrated that while AC-(di-*O*-C14PC)$_2$ monolayer, which adopts a particularly high-ordered structure in the gel phase, shows remarkably high thermotropic transition temperature compared to DTPC bilayer, the fluidity of both phospholipids above the transition temperature is comparable. Nonetheless, the fluorescent dye leakage from inside the AC-(di-*O*-C14PC)$_2$ vesicles in the fluid phase is highly suppressed. The origin of the membrane properties characteristic of AC-(di-*O*-C14PC)$_2$ monolayer is discussed in terms of the single long transmembrane hydrophobic linkage and the diffusional motion of the lipid molecules.

1. Introduction

Biomembrane, a common fundamental structure in the cells of living organisms, is mainly composed of a phospholipid membrane and embedded integral or peripheral membrane proteins. Structural and physical properties of phospholipid membranes significantly vary between the domains of organisms [1–6]. In eukaryotes and bacteria, *sn*-glycerol-3-phosphate-based ester-linked phospholipid molecules together assemble into a bilayer membrane of an inner leaflet and an outer leaflet. On the other hand, archaea, which thrive in various harsh environments, e.g., hot springs and salt lakes, typically utilize phospholipids with distinctive chemical structures. The principal difference is that archaeal phospholipids are built on a backbone of *sn*-glycerol-1-phosphate bearing ether-linkages with a hydrocarbon chain.

An additional striking structural feature reported for some archaeal lipids is that two double-chained ether-linked phospholipid molecules, which generally form bilayer membrane in the aqueous media, are cross-linked through a single or double interlayer bridge of a phytanyl chain to yield amacrocyclic or macrocyclic tetraether phospholipids, respectively [1–6]. Typically, cyclopentene rings of varying proportions are included in the phytanyl chains [1–6]. Such archaea-specific amacrocyclic and macrocyclic tetraether phospholipids have a single or double long

Abbreviations: AC-(di-*O*-C14PC)$_2$, amacrocyclic 1,1'-*O*-octacosamethylene-2,2′-di-*O*-tetradecyl-bis-(*sn-glycero*)-3,3′-diphosphocholine; 6-CF, 6-carboxyfluorescein; di-*O*-C14PC, 1,2-di-*O*-tetradecyl-*sn*-glycero-3-phosphocholine; DPH, diphenylhexatriene; Laurdan, 2-dimethylamino-6-lauroylnaphthalene; WAXD, wide-angle X-ray diffraction.

* Corresponding authors.
** Correspondence to: Masashi Sonoyama, Division of Molecular Science, Faculty of Science and Technology, Gunma University, Kiryu, Gunma 376-8515, Japan.
E-mail addresses: t.takagi@aist.go.jp (T. Takagi), hirotakahashi@gunma-u.ac.jp (H. Takahashi), sonoyama@gunma-u.ac.jp (M. Sonoyama).

https://doi.org/10.1016/j.bbamem.2021.183569
Received 10 November 2020; Received in revised form 14 January 2021; Accepted 27 January 2021
Available online 5 February 2021

phytanyl chain with cyclopentene rings and the two polar head groups at its ends via the ether-linkage with the glycerol moiety. Therefore, it turns out that in the aqueous media, the archaea-specific amacrocyclic and macrocyclic tetraether phospholipids spontaneously form vesicles composed of a "eukaryotic naturally-occurring phospholipid bilayer-like monolayer" membrane. Thus, the transmembrane cross-linkage, the methyl branches, and the cyclopentene rings are the three structural segments characteristic of archaea-specific amacrocyclic and macrocyclic tetraether phospholipids.

In addition to be important targets in the various fields of basic research [7–22], such archaea-specific amacrocyclic and macrocyclic tetraether phospholipids have been attracting much attention as promising materials for pharmaceutical and biomedical applications [23–34]. The highly advantageous properties of such archaea-specific phospholipids are high thermal and mechanical stability and low permeability of membranes. To reveal structural features responsible for the significant archaea phospholipid-specific membrane properties, not only native [15–18,30–34] but also synthetic [7–11,13–14,19–29] amacrocyclic and macrocyclic tetraether phospholipids have been extensively investigated with the use of various biophysical techniques. However, the amacrocyclic and macrocyclic tetraether phospholipids studied in the previous studies are assembled of some of the archaea-specific structural segments such as the covalently cross-linked alkyl chain, the methyl branch, and the cyclopentene ring. Therefore, it is not straightforward to separately clarify effects of the membrane-spanning cross-linkage.

In the present study, a novel amacrocyclic tetraether phospholipid bearing a single transmembrane polymethylene chain that connects two phosphatidylcholine (PC) groups, 1,1'-*O*-octacosamethylene-2,2′-di-*O*-tetradecyl-bis-(*sn*-glycero)-3,3′-diphosphocholine (Fig. 1, AC-(di-*O*-C14PC)$_2$), is developed to elucidate effects of a simple membrane-spanning cross-linkage on membrane properties. The amacrocyclic tetraether phospholipid used corresponds to a dimer of a diether phospholipid 1,2-di-*O*-tetradecyl-*sn*-glycero-3-phosphocholine (di-*O*-C14PC) connected through the cross-linkage between the two PC groups in both inner and outer leaflets of the di-*O*-C14PC bilayer membrane. Therefore, based on detailed comparisons between AC-(di-*O*-C14PC)$_2$ monolayer membrane and di-*O*-C14PC bilayer membrane, it is expected that the effects of a single transmembrane cross-linkage on physical properties are unraveled. The comparative analyses between di-*O*-C14PC bilayer vesicle and AC-(di-*O*-C14PC)$_2$ monolayer vesicle demonstrated that compared to the di-*O*-C14PC vesicle, the leakage of fluorescent compounds inside the AC-(di-*O*-C14PC)$_2$ vesicle is highly suppressed even in the liquid crystalline phase despite high fluidity comparable to the di-*O*-C14PC bilayer.

2. Materials and methods

2.1. Materials

All the reagents for organic synthesis of AC-(di-*O*-C14PC)$_2$ were commercially available and were used without further purification. Di-*O*-C14PC (1,2-Di-*o*-ditetradecyl-*sn*-glycero-3-phosphocholine) was purchased from Avanti Polar Lipids, Inc. Laurdan (6-Dodecanoyl-2-dimethylaminonaphthalene) and DPH (Diphenylhexatriene) were from Molecular Probes, Inc. 6-CF (6-Carboxyfluorescein) was obtained from Tokyo Chemical Industry Co., Ltd. All other chemical reagents used were of research-grade. For efficient preparations of samples for several physicochemical measurements, stock solutions of the phospholipids and the fluorescent dyes except for 6-CF were prepared by dissolving them into chloroform. Methanol was used for the stock solution of 6-CF.

2.2. Organic synthesis of AC-(di-O-C14PC)$_2$

AC-(di-*O*-C14PC)$_2$ (**1**) was synthesized by the following procedures (Scheme 1). Propargyl alcohol protected as THP ether was reacted with 1-bromoundecane by treated with *n*-BuLi in THF-HMPA, and the THP ether was removed to give 2-tetradecyn-1-ol. The isomerization of the alcohol bearing internal triple bond was treated with NaH in 1,3-propandiamine to yield 13-tetradecyn-1-ol having terminal triple bond. The alcohol was mesylated to obtain compound **2** [35–36].

Compound **3** was prepared from (*S*)-(+)-2,2-dimethyl-1,3-dioxolane-4-methanol according to the method described in the literature [37]. Compound **3** was reacted with 1-bromotetradecane in the presence of NaH, the trityl group was deprotected by treated with cat. *p*TsOH, compound **2** was reacted, and the PMB group was removed by DDQ oxidation to provide compound **4** [8,38]. Diol compound having diacetylene group obtained by homo-coupling reaction of compound **4** in the presence of Cu(OAc)$_2$ in pyridine was reduced by treated with Pd(OH)$_2$/C in H_2 atmosphere to obtain compound **5**, and the two hydroxyl groups were converted to phosphocholine groups to get compound **1** [39–40].

2-Bromoethyl phosphorodichloride was prepared from phosphoryl dichloride according to the method of W. J. Hansen et al. [41]. Compound **5** (1.17 g/ 1.21 mmol) was treated with 2-bromoethyl phosphorodichloride (0.90 g/ 3.73 mmol) in benzene containing triethylamine (0.85 mL/6.10 mmol) at room temperature for 18 h, and then the reaction mixture was evaporated. The residue was extracted with $CHCl_3$ after being treated with water at room temperature for 4 h. The solvent was removed under reduce pressure to afford the phosphoryl intermediate. Trimethylamine 30% solution was added to the intermediate in a mixture of [CH_3CN]/[*i*PrOH]/[$CHCl_3$] (5/5/3). The reaction mixture was stirred for 18 h at 60 °C. After the removal of the solvent under reduce pressure, the residue was purified by column chromatography (SiO_2, [$CHCl_3$]:[MeOH]:[H_2O] = 65:35:4 to 65:35:8), Sephadex LH20 (MeOH), and ODS (MeOH)), to give compound **1** (1.08 g/68%).

1: MS (FAB$^+$) *m/z*: 1298 (*M* + H)$^+$. HRMS (FAB$^+$) calcd for $C_{72}H_{151}N_2O_{12}P_2$ (*M* + H)$^+$ 1298.0737: Found 1298.0747. ^{1}H NMR (CD_3OD-$CDCl_3$, TMS): 4.21–4.34 (m, 4H), 3.87 (t, *J* = 5.5 Hz, 4H), 3.65–3.75 (m, 4H), 3.50–3.64 (m, 8H), 3.49–3.37 (m, 6H), 3.29 (s, 18H), 1.46–1.61 (m, 8H), 1.20–1.38 (m, 92H), 0.88 (t, *J* = 6.8 Hz, 6H).

2.3. DSC measurements

A comparison of thermotropic behaviors of phospholipid suspension

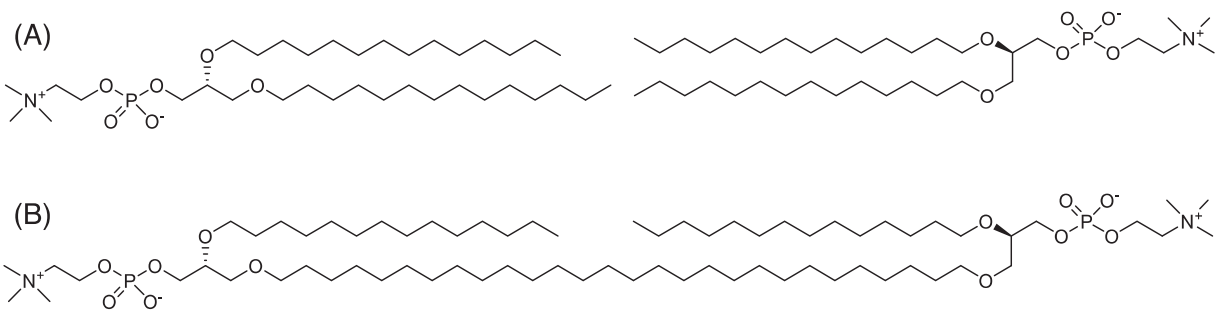

Fig. 1. Chemical structures of (A) di-*O*-C14PC and (B) AC-(di-*O*-C14PC)$_2$. For comparison, di-*O*-C14PC is depicted as a piece of bilayer membrane.

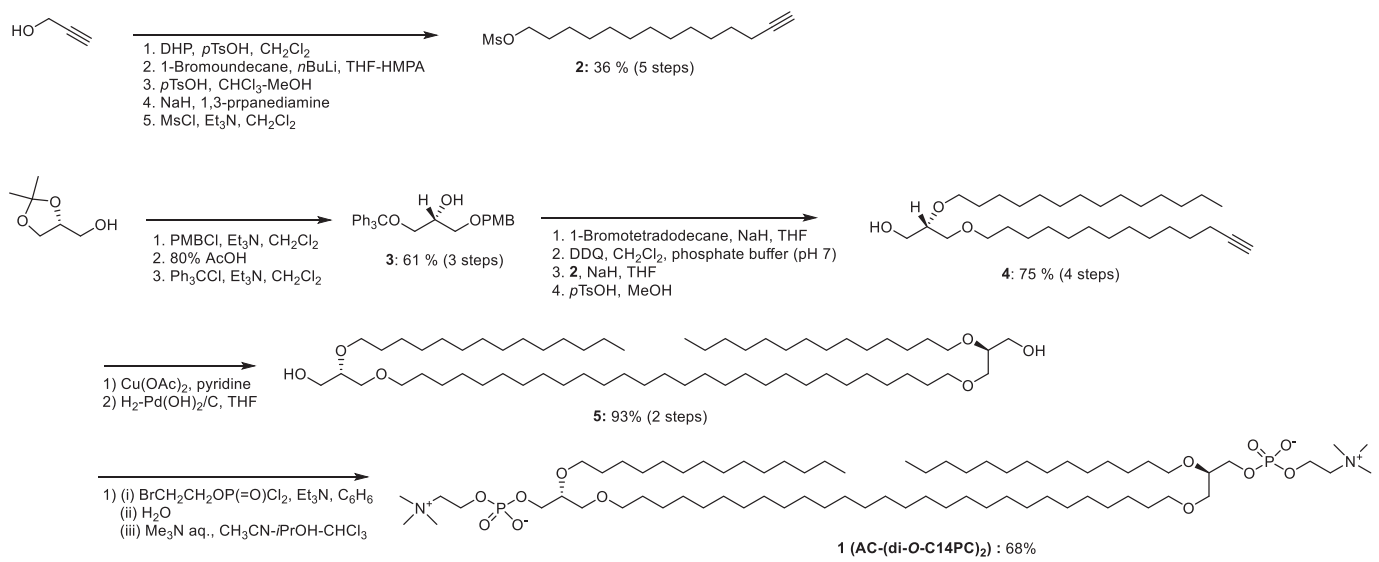

Scheme 1. Synthesis of Amacrocyclic Bisphosphatidylcholine lipid **1**

of AC-(di-*O*-C14PC)$_2$ and di-*O*-C14PC was performed by using DSC measurements. For the measurements, dried films of AC-(di-*O*-C14PC)$_2$ and di-*O*-C14PC were obtained by evaporating the stock solutions under a stream of dry nitrogen and were kept in vacuum for 16 h to remove residual solvents. Multilamellar liposome samples were prepared by suspending the dried phospholipid films in Milli-Q water and sonicating at 55 °C for 1 h. The concentrations of AC-(di-*O*-C14PC)$_2$ and di-*O*-C14PC were 50 and 100 mM, respectively. The thermotropic transition of the phospholipid suspensions was investigated with a SEIKO DSC 6100-Exstar6000 differential scanning calorimeter (Chiba, Japan). The heating rate was 1.0 K min^{-1}. The melting transition of indium was used as a reference for calibration for the instrument.

2.4. WAXD measurements

X-ray diffraction measurements were performed at the bending-magnet beamline BL-6A [42] and BL-10C [43] of the Photon Factory (PF) using synchrotron radiation beams from the PF storage ring at High Energy Accelerator Research Organization, KEK (Tsukuba, Japan). The wavelength of X-ray beam was 0.15 nm (BL-6A) or 0.10 nm (BL-10C). Typical detector-to-sample distances were ~300 mm and ~500 mm for BL-6A and BL-10C, respectively. The distance was determined by analyzing the diffraction patterns of standard sample, silver behenate [44]. The temperature of samples was controlled by a modified differential scanning calorimeter (FP 84, Mettler-Toledo International Inc.) [45]. For X-ray diffraction studies, the samples were pelleted by centrifugation at 18,000*g* for 30 min at 2 °C with a temperature-controlled centrifuge (MX-150, TOMY SEIKO Co. Ltd.). Two-dimensional X-ray diffraction patterns were recorded with an X-ray photon counting pixel array detector PILATUS100K or PILATUS1M (DECTRIS, Switzerland) [42]. Typical exposure time was 20 s.

By using a FIT2D software [46–47], circular integrations were carried out to transform into one-dimensional intensity data from the two-dimensional diffraction image data. In this paper, we used the reciprocal spacing (S), $S = 1/d = 2\sin\theta/\lambda$ (where d is the real spacing, 2θ is the scattering angle, and λ is the wavelength of X-ray) for the horizontal axis to display X-ray diffraction data.

2.5. DPH fluorescence depolarization measurements

Steady-state fluorescence depolarization measurements of DPH in the phospholipid membrane [48–51] was employed to probe differences in the membrane fluidity between AC-(di-*O*-C14PC)$_2$ and di-*O*-C14PC. For measurements of fluorescent dyes of DPH in the phospholipid membrane, the stock solutions of AC-(di-*O*-C14PC)$_2$ and di-*O*-C14PC were mixed with that of the fluorescent dye at the molar ratio of 250:1 and 500:1, respectively, and films of the phospholipid/fluorescent dye mixture were prepared by evaporating the solvent at 40 °C and then drying under the reduced pressure for 3 h. The dried films were suspended with Milli-Q water and vortexed at 60 °C to obtain the suspensions samples for the steady-state fluorescence measurements. The final phospholipid concentrations of the samples are 0.25 and 0.5 mM for AC-(di-*O*-C14PC)$_2$ and di-*O*-C14PC, respectively.

An Edinburgh FS 900 CDT fluorometer (Edinburgh Analytical Instruments) was utilized for fluorescence depolarization measurements of DPH in the phospholipid membrane. The excitation wavelength was 360 nm, and the fluorescence spectra in the wavelength region of 420–440 nm were obtained in the temperature range of 20–70 °C. The anisotropy (r) values were obtained from intensity measurements of vertically and horizontally polarized emissions with vertically polarized excitation (I_{VV} and I_{VH}) and a grating factor G that derives from intensities of vertically and horizontally polarized emissions with horizontally polarized excitation (I_{HV} and I_{HH}). The temperature control was performed with the use of a temperature-controlled water bath (Thermo Scientific NESLAB RTE-7 Circulating Bath).

2.6. Laurdan fluorescence measurements

A polarity-sensitive fluorescent Laurdan was used to reveal the polarity around the hydrophilic/hydrophobic interface region of the phospholipid membrane [52–54]. A film was obtained by evaporation of the mixture of a phospholipid and Laurdan stock solutions with a phospholipid/Laurdan molar ratio of 500:1 under a stream of oxygen-free dry nitrogen. For Laurdan fluorescence measurements, the film of phospholipid and Laurdan was hydrated with Milli-Q water at around 55 °C for about 10 min and was vortexed after the incubation at the final lipid concentration of about 0.5 mM.

A Hitachi F-4500 fluorescence spectrophotometer was employed for measurements of steady-state fluorescence emission spectra in the region of 380 to 650 nm. The excitation wavelength was 361 nm. The temperature was controlled with an accuracy of ~0.01 °C by using a Julabo F25 recirculating chiller. The fluorescence spectral shift was quantitatively evaluated by calculating the generalized polarization (GP) function proposed by Parasassi et al. [52–54].

2.7. Fluorescent dye leakage assay

The dye leakage assay based on an anionic fluorophore 6-CF self-quenching properties [15,55–56] was tested to investigate differences in the permeability of the phospholipid liposomes between AC-(di-*O*-C14PC)$_2$ and di-*O*-C14PC. A previous study by Komatsu and Chong [15] demonstrated that the tight and rigid lipid packing is responsible for the leakage rate of 6-CF. For the preparation of 6-CF-loaded liposomes, phospholipid/dye film samples were prepared by evaporating the mixture of the stock solution of AC-(di-*O*-C14PC)$_2$/di-*O*-C14PC and 6-CF at the molar ratio of 10/5 to 1, respectively, at 40 °C, under a stream of oxygen-free dry nitrogen and were dried under a reduced-pressure for 3 h. Furthermore, dried films were suspended with 10 mM HEPES buffer (pH 7.4) above the phase transition temperatures. After the overnight incubation for hydration at room temperature, the obtained suspension samples were subject to the freeze-thaw cycles several times and centrifugation (4000 *g*, 15 min) twice at 4 °C to obtain 6-CF-loaded unilamellar vesicle and remove residual unloaded fluorescent dyes. The final phospholipid/dye suspension samples used for the dye leakage assay were obtained by suspending the pellet with 10 mM HEPES buffer (pH 7.4) at the final phospholipid concentrations of 2.25 mM for AC-(di-*O*-C14PC)$_2$ and 4.5 mM for di-*O*-C14PC, respectively.

Fluorescence of liposomes loaded with 6-CF was monitored at 520 nm (excitation at 495 nm) with a Hitachi F-4500 spectrofluorometer. The extent of 6-CF efflux was calculated as $(F_t\text{-}F_0)/(F_{100}\text{-}F_0)$, where F_0 and F_t represent the initial fluorescence intensity and the fluorescence intensity at the time t, respectively, and F_{100} is the fluorescence intensity after complete disruption of liposomes by addition of 0.1% Triton X-100. The temperature was controlled by using a Julabo F25 recirculating chiller.

3. Results and discussion

3.1. Thermotropic characterization

DSC measurements were carried out for phospholipid suspensions to reveal differences in thermotropic behaviors of phospholipid membrane between AC-(di-*O*-C14PC)$_2$ and di-*O*-C14PC. As shown in Fig. 2, a remarkably sharp endothermic peak is observed for di-*O*-C14PC at 26.4 ± 0.1 °C, which is in good agreement with the previous report [57]. According to the previous work [57], the DSC peak is attributable to the gel-to-liquid crystalline phase transition ($P_{\beta'} \rightarrow L_\alpha$), which is also supported by the temperature-dependent changes of the WAXD patterns of di-*O*-C14PC shown in Fig. 3A. The transition enthalpy ΔH and entropy ΔS obtained from the DSC data are 22.4 ± 0.9 kJ mol^{-1} and 74.7 ± 3.1 J K^{-1} mol^{-1}, respectively. The thermodynamic values are also very similar to those in the previous work [57].

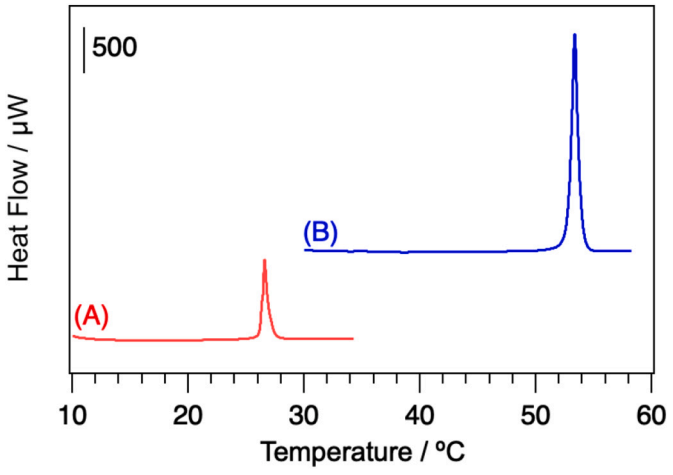

Fig. 2. Differential scanning calorimetric curves of (A) di-*O*-C14PC and (B) AC-(di-*O*-C14PC)$_2$. Thermograms are offset vertically for clarity.

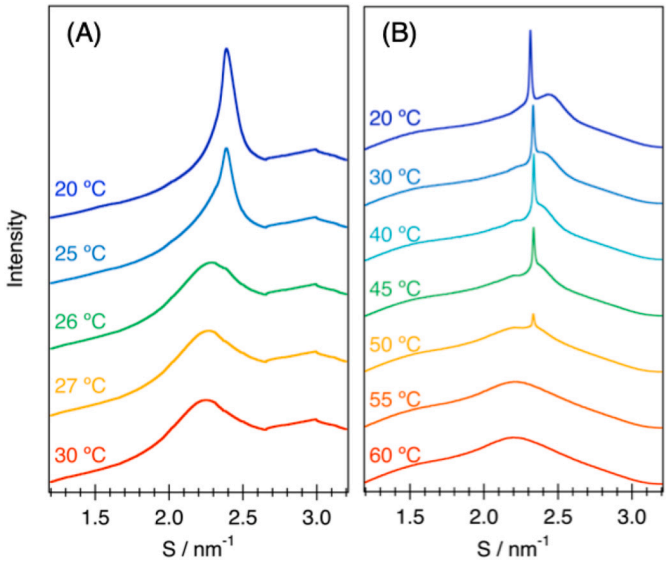

Fig. 3. Wide-angel X-ray diffraction patterns of (A) di-*O*-C14PC and (B) AC-(di-*O*-C14PC)$_2$. Peaks are offset vertically for clarity.

For AC-(di-*O*-C14PC)$_2$, on the other hand, an endothermic peak appears at 53.4 ± 0.1 °C, which is as high as ~27 °C compared to di-*O*-C14PC. In order to investigate what is responsible for the endothermic peak, WAXD measurements were performed for the AC-(di-*O*-C14PC)$_2$ membrane in the temperature range of 20–60 °C. The WAXD pattern of AC-(di-*O*-C14PC)$_2$ at 20 °C is composed of a remarkably sharp peak at S = 2.31 nm^{-1} with a broad one centered at S = 2.45 nm^{-1} (Fig. 3B). Upon heating to 50–55 °C, the characteristic WAXD peak dramatically changes to a broad featureless one, indicating that the endothermic peak at 53.4 ± 0.1 °C in the DSC thermogram (Fig. 2B) is due to the chain-melting transition. The transition enthalpy and entropy of the AC-(di-*O*-C14PC)$_2$ membrane were estimated from the DSC data and are shown in Table 1. Because AC-(di-*O*-C14PC)$_2$ molecules assemble into a monolayer membrane, the thermodynamic values per molecule obtained for the AC-(di-*O*-C14PC)$_2$ membrane are approximately doubled compared to those obtained for bilayer membranes of usual phospholipids (e.g., dimyristoylphosphatidylcholine). Therefore, halves of the thermodynamic values for the AC-(di-*O*-C14PC)$_2$ membrane are also listed as converted values for comparison. The converted ΔH and entropy ΔS for AC-(di-*O*-C14PC)$_2$ are 30.8 ± 0.8 kJ mol^{-1} and 94.2 ± 2.7 J K^{-1} mol^{-1}, respectively, that are higher than di-*O*-C14PC.

Of particular note is that the marked sharp peak at S = 2.31 nm^{-1} appears for AC-(di-*O*-C14PC)$_2$ in the gel phase. The full width at half maximum for the sharp peak of AC-(di-*O*-C14PC)$_2$ at 20 °C is roughly estimated to be ~0.016 nm^{-1} from the diffraction peak, which is approximately an order of magnitude smaller than that for the central peak at S = 2.34 nm^{-1} for di-*O*-C14PC at 20 °C (~0.14 nm^{-1}, Fig. 3A). The remarkable difference in the width of the dominant endothermic peak at 20 °C strongly suggests that in the AC-(di-*O*-C14PC)$_2$ membrane,

Table 1
Thermodynamic properties for the phase transition of di-*O*-C14PC and AC-(di-*O*-C14PC)$_2$. Parenthesized values of ΔH and ΔS for AC-(di-*O*-C14PC)$_2$ are the values reduced to half for comparison with di-*O*-C14PC.

Lipid	*Tm* (°C)	ΔH (kJ mol^{-1})	ΔS (J K^{-1} mol^{-1})
di-*O*-C14PC	26.6 ± 0.1	22.4 ± 0.9	74.7 ± 3.1
AC-(di-*O*-C14PC)$_2$	53.4 ± 0.1	61.5 ± 1.5 (30.8 ± 0.8)	188.3 ± 5.5 (94.2 ± 2.7)

a much more highly ordered structure is formed in the hydrophobic region compared to di-*O*-C14PC. It is reasonable to conclude that the highly ordered structure formed in the AC-(di-*O*-C14PC)$_2$ membrane is attributable to a single membrane-spanning linkage of a long methylene chain of $(CH_2)_{28}$ between the phosphatidylcholine groups in the inner and the outer sides of the membrane and contributes to the above-mentioned significant difference of ~27 °C in *T*m between AC-(di-*O*-C14PC)$_2$ and di-*O*-C14PC. Preliminary small-angle X-ray diffraction analyses of AC-(di-*O*-C14PC)$_2$ membrane at 2 °C demonstrated that the membrane thickness is ~3.8 nm. The value of the thickness is very similar to that of the AC-(di-*O*-C14PC)$_2$ monolayer membrane expected from its chemical structure, strongly suggesting that AC-(di-*O*-C14PC)$_2$ membrane in the gel phase does not adopt the interdigitated structure, unlike di-*O*-C14PC bilayer (Tsuchida et al., unpublished results). Therefore, it is plausible that the long transmembrane hydrocarbon segments are in the all-*trans* planar zigzag conformation, which could induce the ordering of the AC-(di-*O*-C14PC)$_2$ membrane. The tentative picture of the AC-(di-*O*-C14PC)$_2$ will be addressed by vibrational spectroscopy in the near future. On the other hand, the less ordered structure and lower *T*m of di-*O*-C14PC bilayer membrane may be attributable to weaker interlayer interaction, compared to the covalently bonded long hydrophobic segment of AC-(di-*O*-C14PC)$_2$.

3.2. Membrane fluidity

The membrane fluidity was probed by steady-state fluorescence depolarization measurements of DPH in the temperature range of 20–70 °C. In Fig. 4, thermal changes of the anisotropy (*r*) values for DPH in the AC-(di-*O*-C14PC)$_2$ membrane are shown with those in the di-*O*-C14PC membrane for comparison. The *r*-value for di-*O*-C14PC in the temperature range of the gel phase is almost constant at ~0.34, which is very similar to those for 1,2-dimyristoyl-*sn*-glycero-3-phosphocholine (DMPC) in the gel phase, the ester-linked phosphatidylcholine corresponding to di-*O*-C14PC, indicating that in the gel phase, rotational depolarization of DPH molecules is significantly limited in the di-*O*-C14PC membrane like in the DMPC membrane [48–49]. Upon temperature elevation above *T*m, however, the value of the fluorescence anisotropy dramatically decreases to ~0.15, which is at the same level as the DMPC membrane in the fluid phase [48–49], showing that fluidity of phospholipid membrane is mostly independent of whether the hydrophobic chains are linked to the glycerol moiety through the ester or the ether bond. Moreover, the r-value of the AC-(di-*O*-C14PC)$_2$ membrane changes in a very similar temperature-dependent manner; the anisotropy value, which is almost constant at ~0.32 in the gel phase, sharply decreases at the temperature of the endothermic peak and gradually diminishes to ~0.14 with further temperature elevation. These experimental results demonstrate that the monolayer membrane of the amacrocyclic tetraether phosphocholine AC-(di-*O*-C14PC)$_2$ undergoes the thermotropic transition from the gel phase to the liquid crystalline phase, and the fluidity of AC-(di-*O*-C14PC)$_2$ after the transition is comparable to that of the bilayer membrane of the corresponding double-chained diether phosphocholine di-*O*-C14PC.

As an essential membrane property closely related to membrane fluidity, the polarity around the hydrophilic/hydrophobic membrane interface region, which strongly reflects water penetration induced by the phase transition, was also probed by a polarity-sensitive fluorescent Laurdan. The GP parameters obtained from fluorescence spectral changes for Laurdan in the AC-(di-*O*-C14PC)$_2$ and di-*O*-C14PC membrane are shown in Fig. 5. The GP values for di-*O*-C14PC are mostly constant at ca. 0.3 in the temperature range of the gel phase, which is significantly small compared to those for DMPC [58]. The significant differences in the GP values between di-*O*-C14PC and DMPC demonstrate that the polarity around the interface region of the di-*O*-C14PC bilayer is higher than that of DMPC. The origin of the polarity difference in the hydrophobic/hydrophilic interface is attributable to the chemical structural variations of the ester or the ether bond and/or the accessibility of water molecules [59], which would result in some perturbation to the molecular interaction between phospholipids. It should be noted that between di-*O*-C14PC and DMPC in the gel phase, the Laurdan fluorescence revealed very different properties in the hydrophilic/hydrophobic membrane interface, while no significant variations in the transmembrane region were demonstrated by DPH fluorescence as mentioned above. These experimental results strongly suggest that the double-chained ester-linked and ether-linked PCs bearing the hydrocarbon segment with the same chain length exhibit similar structural and physical properties for the hydrophobic core region, but different

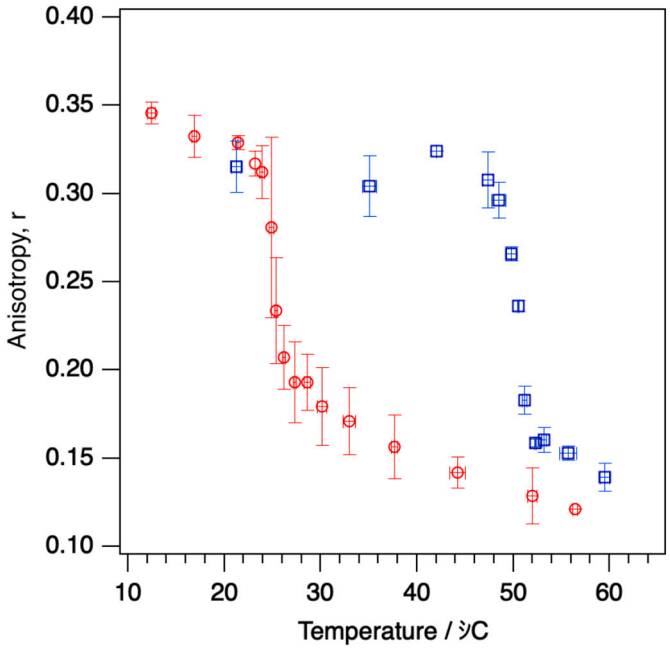

Fig. 4. Anisotropy values of DPH in di-*O*-C14PC (red circles) and AC-(di-*O*-C14PC)$_2$ (blue squares) as a function of temperature.

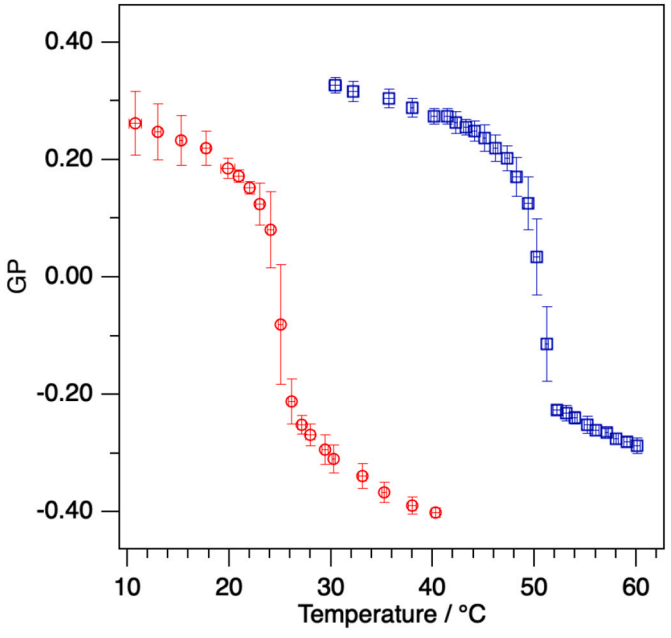

Fig. 5. Generalized polarization (GP) values calculated form Laurdan fluorescence intensities at 440 and 490 in di-*O*-C14PC (red circles) and AC-(di-*O*-C14PC)$_2$ (blue squares) as a function of temperature.

polarity-related properties for the hydrophilic/hydrophobic interface. Furthermore, the GP values for AC-(di-*O*-C14PC)$_2$ in the gel phase are very similar to those for di-*O*-C14PC. This indicates that irrespective of the single transmembrane alkyl linkage between the two glycerophosphate head groups, which induces more ordered chain packing inside the phospholipid membrane as indicated by the WAXD measurements, there are no significant differences in the polarity of the hydrophilic/hydrophobic membrane interface region between AC-(di-*O*-C14PC)$_2$ and di-*O*-C14PC.

In the temperature range of the phase transition, however, both di-*O*-C14PC and AC-(di-*O*-C14PC)$_2$ showed a remarkable drop in the GP values, followed by a gradual decrease to ca. -0.4 at higher temperatures. The dramatic falls of GP to ca. -0.4 indicate that the polarity of the hydrophilic/hydrophobic interface region of the AC-(di-*O*-C14PC)$_2$ membrane becomes higher, which is attributable to enhancement of membrane fluidity by the gel-to-liquid crystalline phase transition. Of note is that compared to DMPC, the GP values for both AC-(di-*O*-C14PC)$_2$ and di-*O*-C14PC in the fluid phase are much smaller, that is, the interface region of the AC-(di-*O*-C14PC)$_2$ and di-*O*-C14PC membrane exhibit highly polar character, which is in the very similar situation to the gel phase as mentioned before.

3.3. Fluorescent dye leakage assay

Dye leakage assay based on 6-CF self-quenching properties was employed to probe the entrapping capability of water-soluble substances inside phospholipid liposomes, which is directly related to the permeability of the phospholipid membrane. A previous study on the membrane permeability of macrocyclic bipolar tetraether lipids from Thermoacidophilic Archaebacterium *Sulfolobus acidocaldarius* revealed that the 6-CF low leakage rate is attributable to the tight and rigid lipid packing and the negative charges on the membrane surface [15]. The extents of 6-CF leakage for AC-(di-*O*-C14PC)$_2$ and di-*O*-C14PC were investigated at 10, 35, and 60 °C to reveal differences between the phase behaviors of phospholipid membrane as well as the two kinds of ether-linked phospholipids. The results are shown in Fig. 5.

At 10 °C in the gel phase for both AC-(di-*O*-C14PC)$_2$ and di-*O*-C14PC, 6-CF leakage is highly suppressed at the same level irrespective of the chemical structural difference between the two kinds of phospholipids, which is due to the limited lateral and rotational diffusion of phospholipid molecules. However, upon temperature elevation to 35 °C, the extent of the fluorescent dye leakage remarkably increases to nearly a half for di-*O*-C14PC in the liquid crystalline phase. In contrast, AC-(di-*O*-C14PC)$_2$ shows no significant changes at the level of less than 10% even after the temperature elevation, which is readily explained by the experimental results that the AC-(di-*O*-C14PC)$_2$ membrane adopts the gel phase at the temperature.

As shown in Fig. 6, a further increase to 60 °C in temperature leads to a tremendous loss of 6-CF up to ~40% inside the AC-(di-*O*-C14PC)$_2$ vesicle, which is attributable to the membrane fluidity induced by the phase transition from the gel phase to the liquid crystalline phase. It is of significant note that the extent of the 6-CF leakage for the AC-(di-*O*-C14PC)$_2$ membrane is highly suppressed compared to the di-*O*-C14PC membrane, where more than twice fluorescent dye molecules leak from the vesicle. These experimental results strongly suggest that even in the fluid phase, AC-(di-*O*-C14PC)$_2$ phospholipid molecules do not diffuse freely, unlike di-*O*-C14PC, but interact with each other to some extent. The peculiar membrane properties of AC-(di-*O*-C14PC)$_2$ in the liquid crystalline phase, which are reasonably ascribed to a single membrane-spanning linkage between the inner and the outer leaflets, are discussed in the next section.

3.4. Effect of a single membrane-spanning linkage on membrane properties

Remarkable physical properties of the AC-(di-*O*-C14PC)$_2$ monolayer

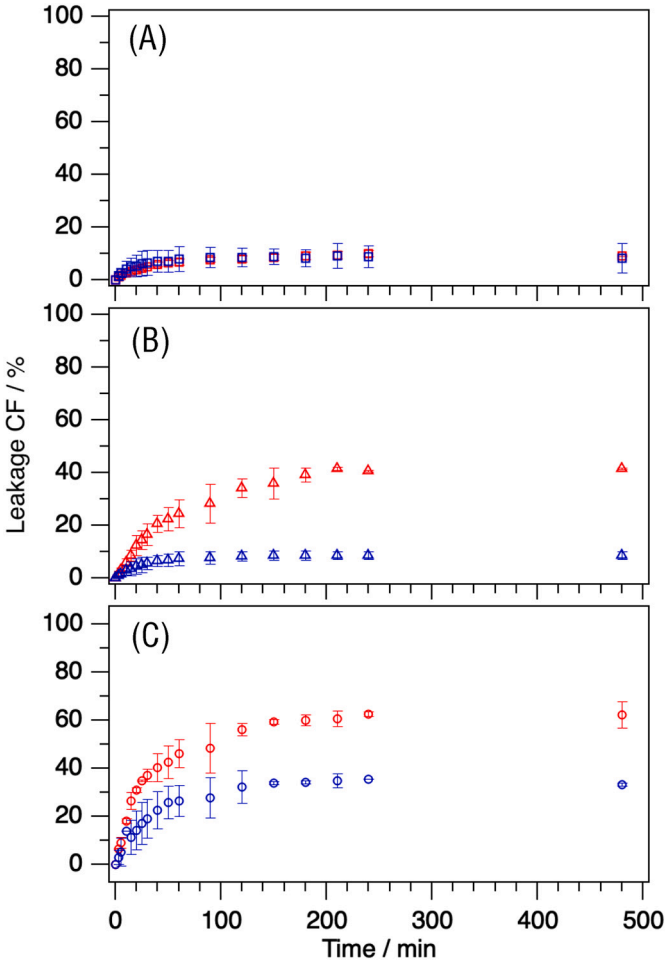

Fig. 6. Time courses of 6-CF leakage from liposome of AC-(di-*O*-C14PC)$_2$ (blue) and di-*O*-C14PC (red) at (A) 10 °C, (B) 35 °C and (C) 60 °C.

revealed by comparison with the di-*O*-C14PC bilayer are summarized as follows: (a) formation of significantly highly ordered structure in the gel phase, (b) dramatic temperature elevation of the thermotropic transition, (c) fluidity in the liquid crystalline phase comparable to the di-*O*-C14PC bilayer and (d) remarkable leakage suppression of substances entrapped inside vesicles in the fluid phase. The very high transition temperature of the AC-(di-O-C14PC)$_2$ monolayer membrane can be discussed in connection with the remarkably high order in its membrane structure. As stated in Section 3.1, the unusual sharp WAXD peak observed for AC-(di-*O*-C14PC)$_2$ demonstrates that the highly ordered chain structure is formed in the transmembrane region, which is unique as phospholipid membrane bearing bulky polar head group like PC. It is reasonable to infer that the most plausible origin for the extraordinarily high structural order of AC-(di-*O*-C14PC)$_2$ monolayer membrane is the transmembrane linkage via the extended octacosamethylene group between the head groups on the opposite sides with each other. A single layer of AC-(di-*O*-C14PC)$_2$ formed through the covalent interlayer linkage between di-*O*-C14PC molecules behaves in a unified manner, which leads to the high structural order in the transmembrane region. On the other hand, two independent layers of di-*O*-C14PC formed by the noncovalent intermolecular interaction in the lateral direction assemble to common lipid bilayer membranes through the vertical noncovalent interlayer interaction, which results in the less ordered di-*O*-C14PC membrane.

As stated in Sections 3.1 and 3.2, highly ordered AC-(di-*O*-C14PC)$_2$ monolayer membrane undergoes the thermotropic transition from the gel phase to the liquid crystalline phase like ordinary phospholipid

bilayer membrane, although the transition temperature is remarkably higher than its corresponding bilayer membrane of di-*O*-C14PC. Of significant note is that fluorescence-probed measurements with DPH and Laurdan demonstrated that the AC-(di-*O*-C14PC)$_2$ monolayer shows fluidic characters comparable to the di-*O*-C14PC bilayer membrane. The fluidic property of phospholipid membrane fundamentally derives from spontaneous lateral and rotational diffusion of phospholipid molecules. In the bilayer membrane, while the lateral and rotational movements of phospholipid molecules are confined in either the inner or the outer leaflet, the spontaneous transverse diffusion between the different leaflets, i.e., the flip-flop, is restricted in a significant way in the absence of phospholipid-transporting membrane proteins. On the other hand, the AC-(di-*O*-C14PC)$_2$ membrane comprises a single layer of the large transmembrane molecules. Although the diffusional behavior of the AC-(di-O-C14PC)$_2$ molecules in the membrane is unknown, it can be deduced from the 6-CF leakage assay experimental results.

It should be noted that in the liquid crystalline phase, the leakage of water-soluble fluorescent 6-CF molecules inside AC-(di-*O*-C14PC)$_2$ monolayer vesicles is much more highly suppressed compared to di-*O*-C14PC bilayer vesicles, even though DPH and Laurdan fluorescence measurements demonstrated that AC-(di-*O*-C14PC)$_2$ molecules have high fluidic property comparable to di-*O*-C14PC. It is reasonably mentioned that the lateral diffusion of phospholipid molecules plays a central role in the leakage of the water-soluble dye molecules 6-CF from inside vesicles because temporal fractures in the membrane are required for the water-soluble molecules to transect the hydrophobic lipid layer. Therefore, while the lateral diffusion of AC-(di-*O*-C14PC)$_2$ molecules is controlled at the moderately low level even in the liquid crystalline phase, which results in the remarkable suppression of the 6-CF leakage, their rotational diffusion is sufficiently activated above the transition temperature, which is the essential origin of the fluidic monolayer membrane comparable to the di-*O*-C14PC bilayer. The characteristic membrane properties of AC-(di-*O*-C14PC)$_2$ are attributable to the extended transmembrane bridge via the octacosamethylene group between the polar head groups on the opposite sides with each other. Our ongoing X-ray diffraction studies on the membrane structure of AC-(di-*O*-C14PC)$_2$ strongly suggest that the decrease in the membrane thickness by the thermotropic phase transition is highly suppressed compared to common bilayer phospholipid membranes, which may indicate that the transmembrane cross-linkage props the monolayer membrane even in the liquid crystalline phase (Tsuchida et al., unpublished results).

As mentioned above, the present study demonstrated that the single interlayer cross-linkage via the linear polymethylene chain induces the highly ordered membrane structure in the gel phase and the remarkable temperature elevation of the thermotropic transition to 53.4 °C compared to the corresponding bilayer membrane of di-*O*-C14PC. Supposing that double interlayer cross-linkages via the linear polymethylene chain are introduced to provide macrocyclic tetraether phospholipid molecules, which is the general backbone structure of naturally occurring archaeal bipolar tetraether lipid, it is inferred that the phase transition temperature of the macrocyclic tetraether phospholipid membrane is further elevated from 53.4 °C. Such a high thermotropic transition temperature leads to the highly rigid phospholipid membrane even at substantially high temperatures. Too much high rigidity would not be suitable for various biological functions on the membrane. As reported in the previous works [15–18,30–34], long transmembrane cross-linkages of native archaeal macrocyclic tetraether lipids contain the phytanyl chain and the cyclopentane ring moieties in some cases, which would moderately loosen the molecular packing, decrease in the phase transition temperature and yield well-suited functional fields for membrane proteins.

4. Conclusions

The monolayer formation of phospholipid membrane by introducing the long membrane-spanning linkage via the polymethylene chain induced some unique membrane properties that are not observed for typical phospholipid bilayer membranes. In particular, the high ability for entrapping water-soluble substances inside phospholipid vesicles even in the fluidic phase is a significant feature of the amacrocyclic tetraether bisphosphatidylcholine lipid, which is presumably the essential membrane property of archaea that can survive in the extreme environment.

Declaration of competing interest

The authors declare that they have no known competing financial interests or personal relationships that could have appeared to influence the work reported in this paper.

Acknowledgements

This work was supported in part by Grants-in-Aid for Scientific Research (KAKENHI: 15K05558 and 20K06573 to M.S., 18K06568 to T. T., and 19K03762 to H.T.) from the Japan Society for the Promotion of Science (JSPS). X-ray diffraction experiments were carried out under the approval of the Photon Factory Program Advisory Committee (Proposals No. 20013G675 and 2018G095). The authors wish to thank Professors N. Shimizu and N. Igarashi and the SAXS beamline staff of Photon Factory for their kind assistance.

References

[1] M. Kates, The phytanyl ether-linked polar lipids and isoprenoid neutral lipids of extremely halophilic bacteria, Prog. Chem. Fats Other Lipids 15 (1977) 301–342, https://doi.org/10.1016/0079-6832(77)90011-8.
[2] M. De Rosa, A. Gambacorta, A. Gliozzi, Structure, biosynthesis, and physicochemical properties of archaebacterial lipids, Microbiol. Rev. 50 (1986) 70–80.
[3] Y. Koga, M. Nishihara, H. Morii, M. Akagawa-Matsushita, Ether polar lipids of methanogenic bacteria: structures, comparative aspects, and biosynthesis, Microbiol. Rev. 57 (1993) 164–182.
[4] Y. Koga, H. Morii, M. Akagawa-Matsushita, M. Ohga, Correlation of polar lipid composition with 16s rrna phylogeny in methanogens. Further analysis of lipid component parts, Biosci. Biotech. Biochem. 62 (1998) 230–236, https://doi.org/10.1271/bbb.62.230.
[5] Y. Koga, H. Morii, Recent advances in structural research on ether lipids from archaea including comparative and physiological aspects, Biosci. Biotechnol. Biochem. 69 (2005) 2019–2034.
[6] A. Caforio, A.J.M. Driessen, Archaeal phospholipids: structural properties and biosynthesis, Biochim. Biophys. Acta 1862 (2017) 1325–1339, https://doi.org/10.1016/j.bbalip.2016.12.006.
[7] R.A. Moss, T. Fujita, Y. Okumura, Dynamics of a bolaamphiphilic lipid in a bilayer liposome, Langmuir 7 (1991) 2415–2418, https://doi.org/10.1021/la00059a001.
[8] J.M. Kim, D.H. Thompson, Tetraether bolaform amphiphiles as models of archaebacterial membrane lipids: synthesis, differential scanning calorimetry, and monolayer studies, Langmuir 8 (1992) 637–644, https://doi.org/10.1021/la00038a056.
[9] D.H. Thompson, K.F. Wong, R. Humphry-Baker, J.J. Wheeler, J.M. Kim, S. B. Rananavare, Tetraether bolaform amphiphiles as models of archaebacterial membrane lipids: Raman spectroscopy, phosphorus-31 NMR, x-ray scattering, and electron microscopy, J. Am. Chem. Soc. 114 (1992) 9035–9042, https://doi.org/10.1021/ja00049a040.
[10] A.P. Patwardhan, D.H. Thompson, Novel flexible and rigid tetraether amacrocyclic and macrocyclic bisphosphocholines: Synthesis and monolayer properties, Langmuir 16 (2000) 10340–10350, https://doi.org/10.1021/la001104q.
[11] K. Yamauchi, K. Doi, M. Kinoshita, F. Kii, H. Fukuda, Archaebacterial lipid models: highly salt-tolerant membranes from 1,2-diphytanylglycero-3-phosphocholine, Biochim. Biophys. Acta 1110 (1992) 171–177, https://doi.org/10.1016/0005-2736(92)90355-P.
[12] Q. Fan, A. Relini, D. Cassinadri, A. Gambacorta, A. Gliozzi, Stability against temperature and external agents of vesicles composed of archaeal bolaform lipids and egg PC, Biochim. Biophys. Acta 1240 (1992) 83–88, https://doi.org/10.1016/0005-2736(95)00157-X.
[13] T. Eguchi, K. Ibaragi, K. Kakinuma, Total synthesis of archaeal 72-membered macrocyclic tetraether lipids, J. Org. Chem. 63 (1998) 2689–2698, https://doi.org/10.1021/jo972328p.
[14] K. Arakawa, H. Kano, T. Eguchi, Y. Nishiyama, K. Kakinuma, Significance of the 72-membered macrocyclic structure found in archaeal membrane lipids: model studies of the macrocyclic tetraether diphospholipids by calorimetric, 31P NMR, and electron microscopic analyses, Bull. Chem. Soc. Jpn. 72 (1999) 1575–1581, https://doi.org/10.1246/bcsj.72.1575.

[15] H. Komatsu, P.L.-G. Chong, Low permeability of liposomal membranes composed of bipolar tetraether lipids from thermoacidophilic archaebacterium *Sulfolobus acidocaldarius*, Biochem. 37 (1998) 107–115, https://doi.org/10.1021/bi972163e.

[16] J.L. Gabriel, P.L.-G. Chong, Molecular modeling of archaebacterial bipolar tetraether lipid membranes, Chem. Phys. Lipids 105 (2000) 193–200, https://doi.org/10.1016/S0009-3084(00)00126-2.

[17] P.L.-G. Chong, R. Ravindra, M. Khurana, V. English, R. Winter, Pressure perturbation and differential scanning calorimetric studies of bipolar tetraether liposomes derived from the thermoacidophilic archaeon *Sulfolobus acidocaldarius*, Biophys. J. 89 (2005) 1841–1849, https://doi.org/10.1529/biophysj.105.063933.

[18] P.L.-G. Chong, Archaebacterial bipolar tetraether lipids: physico-chemical and membrane properties, Chem. Phys. Lipids 163 (2010) 253–265, https://doi.org/10.1016/j.chemphyslip.2009.12.006.

[19] T. Koyanagi, G. Leriche, D. Onofrei, G.P. Holland, M. Mayer, J. Yang, Cyclohexane rings reduce membrane permeability to small ions in archaea-inspired tetraether lipids, Angew. Chem. Int. Ed. 55 (2016) 1890–1893, https://doi.org/10.1002/anie.201510445.

[20] T.B.H. Schroeder, G. Leriche, T. Koyanagi, M.A. Johnson, K.N. Haengel, O. M. Eggenberger, C.L. Wang, Y.H. Kim, K. Diraviyam, D. Sept, J. Yang, M. Mayer, Effects of lipid tethering in extremophile-inspired membranes on H(+)/OH(-) flux at room temperature, Biophys. J. 110 (2016) 2430–2440, https://doi.org/10.1016/j.bpj.2016.04.044.

[21] V. Paolucci, G. Leriche, T. Koyanagi, J. Yang, Evaluation of tetraether lipid-based liposomal carriers for encapsulation and retention of nucleoside-based drugs, Bioorg. Med. Chem. Lett. 27 (2017) 4319–4322, https://doi.org/10.1016/j.bmcl.2017.08.032.

[22] G. Leriche, D. Stengel, D. Onofrei, T. Koyanagi, G.P. Holland, J. Yang, Fusion of bipolar tetraether lipid membranes without enhanced leakage of small molecules, Sci. Rep. 9 (2019) 19359, https://doi.org/10.1038/s41598-019-55494-z.

[23] T. Benvegnu, M. Brard, D. Plusquellec, Archaeabacteria bipolar lipid analogues: structure, synthesis and lyotropic properties, Curr. Opin. Colloid Interface Sci. 8 (2004) 469–479, https://doi.org/10.1016/j.cocis.2004.01.005.

[24] M. Brard, W. Richter, T. Benvegnu, D. Plusquellec, Synthesis and supramolecular assemblies of bipolar archaeal glycolipid analogues containing a cis-1,3-disubstituted cyclopentane ring, J. Am. Chem. Soc. 126 (2004) 10003–10012, https://doi.org/10.1021/ja049805n.

[25] T. Benvegnu, G. Réthoré, M. Brard, W. Richter, D. Plusquellec, Archaeosomes based on novel synthetic tetraether-type lipids for the development of oral delivery systems, Chem. Commun. 44 (2005) 5536–5538, https://doi.org/10.1039/B511440C.

[26] M. Brard, C. Lainé, G. Réthoré, I. Laurent, C. Neveu, L. Lemiègre, T. Benvegnu, Synthesis of archaeal bipolar lipid analogues: a way to versatile drug/gene delivery systems, J. Org. Chem. 72 (2007) 8267–8279, https://doi.org/10.1021/jo071181r.

[27] T. Benvegnu, L. Lemiègre, S. Cammas-Marion, Archaeal lipids: innovative materials for biotechnological applications, Eur. J. Org. Chem. 28 (2008) 4725–4744, https://doi.org/10.1002/ejoc.200800452.

[28] A. Jacquemet, J. Barbeau, L. Lemiègre, T. Benvegnu, Archaeal tetraether bipolar lipids: structures, functions and applications, Biochimie 91 (2009) 711–717, https://doi.org/10.1016/j.biochi.2009.01.006.

[29] A. Jiblaoui, J. Barbeau, T. Vivès, P. Cormier, V. Glippa, B. Cosson, T. Benvegnu, Folate-conjugated stealth archaeosomes for the targeted delivery of novel antitumoral peptides, RSC Adv. 6 (2016) 75234–75241, https://doi.org/10.1039/C6RA15713K.

[30] J. Parmentier, B. Thewes, F. Gropp, G. Fricker, Oral peptide delivery by tetraether lipid liposomes, Int. J. Pharm. 415 (2011) 150–157, https://doi.org/10.1016/j.ijpharm.2011.05.066.

[31] J. Parmentier, M.M.M. Becker, U. Heintz, G. Fricker, Stability of liposomes containing bio-enhancers and tetraether lipids in simulated gastro-intestinal fluids, Int. J. Pharm. 405 (2011) 210–217, https://doi.org/10.1016/j.ijpharm.2010.12.005.

[32] J. Parmentier, G. Hofhaus, S. Thomas, L.C. Cuesta, F. Gropp, R. Schröder, K. Hartmann, G. Fricker, Improved oral bioavailability of human growth hormone by a combination of liposomes containing bio-enhancers and tetraether lipids and omeprazole, J. Pharm. Sci. 103 (2014) 3985–3993, https://doi.org/10.1002/jps.24215.

[33] P. Uhl, S. Pantze, P. Storck, J. Parmentier, D. Witzigmann, G. Hofhaus, J. Huwyler, W. Mier, G. Fricker, Oral delivery of vancomycin by tetraether lipid liposomes, Eur. J. Pharm. Sci. 108 (2017) 111–118, https://doi.org/10.1016/j.ejps.2017.07.013.

[34] G. Mahmoud, J. Jedelská, B. Strehlow, U. Bakowsky, Bipolar tetraether lipids derived from thermoacidophilic archaeon *Sulfolobus acidocaldarius* for membrane stabilization of chlorin e6 based liposomes for photodynamic therapy, Eur. J. Pharm. Biopharm. 95 (2015) 88–98, https://doi.org/10.1016/j.ejpb.2015.04.009.

[35] S.R. Macaulay, Isomerization of internal triple bonds of alkyn-1-ols with sodium hydride in 1,3-diaminopropane, J. Org. Chem. 45 (1980) 734–735, https://doi.org/10.1021/jo01292a042.

[36] J.F. Carvalho, G.D. Prestwich, Synthesis of ω-tritiated and ω-fluorinated analogs of the trail pheromone of subterranean termites, J. Org. Chem. 49 (1984) 1251–1258, https://doi.org/10.1021/jo00181a023.

[37] K. Miyawaki, T. Takagi, M. Shibakami, Efficient Synthesis of parallel cyclobolaphiles having two diacetylenes: Mimetics of archaeal membrane lipids, Synlett 2002 (2002) 1326–1328, https://doi.org/10.1055/s-2002-32987.

[38] A.P. Patwardhan, D.H. Thompson, Novel flexible and rigid tetraether amacrocyclic and macrocyclic bisphosphocholines: synthesis and monolayer properties, Langmuir 16 (2000) 10340–10350.

[39] N. Hebert, A. Beck, R.B. Lennox, G. Just, A new reagent for the removal of the 4-methoxybenzyl ether: application to the synthesis of unusual macrocyclic and bolaform phosphatidylcholines, J. Org. Chem. 57 (1992) 1777–1783, https://doi.org/10.1021/jo00032a033.

[40] T. Takagi, K. Takai, T. Baba, T. Kanamori, Synthesis of phospholipids containing perfluorooctyl group and their interfacial properties, J. Fluor. Chem. 128 (2007) 133–138, https://doi.org/10.1016/j.jfluchem.2006.10.020.

[41] W.J. Hansen, R. Murari, Y. Wedmid, W.J. Baumann, An improved procedure for the synthesis of choline phospholipids via 2-bromoethyl dichlorophosphate, Lipids 17 (1982) 453–459, https://doi.org/10.1007/BF02535226.

[42] N. Shimizu, T. Mori, N. Igarashi, H. Ohta, Y. Nagatani, T. Kosuge, K. Ito, Refurbishing of small-angle X-ray scattering beamline, BL-6A at the Photon Factory, J. Phys. Conf. Ser. 425 (2013) 202008, https://doi.org/10.1088/1742-6596/425/20/202008.

[43] N. Igarashi, Y. Watanabe, Y. Shinohara, Y. Inoko, G. Matsuba, H. Okuda, T. Mori, K. Ito, Upgrade of the small angle X-ray scattering beamlines at the photon factory, J. Phys. Conf. Ser. 272 (2011), 012026 https://doi.org/10.1088/1742-6596/272/1/012026.

[44] T.C. Huang, H. Toraya, T.N. Blanton, Y. Wu, X-ray powder diffraction analysis of silver behenate, a possible low-angle diffraction standard, J. Appl. Crystallogr. 26 (1993) 180–184, https://doi.org/10.1107/S0021889892009762.

[45] H. Takahashi, S. Matuoka, Y. Amemiya, I. Hatta, Simultaneous differential scanning calorimetry and time-resolved X-ray diffraction of lipid-water system. I. Relationship between chain melting and endothermic heat at the main transition of a dipalmitoylphosphatidylcholine-water system, Chem. Phys. Lipids 76 (1995) 115–121, https://doi.org/10.1016/0009-3084(94)02428-8.

[46] E.F. Eikenberry, Ch. Brönnimann, G. Hülsen, H. Toyokawa, R. Horisberger, B. Schmitt, C. Schulze-Briese, T. Tomizaki, PILATUS: a two-dimensional X-ray detector for macromolecular crystallography, Nucl. Instrum. Methods Phys. Res. A 501 (2003) 260–266, https://doi.org/10.1016/S0168-9002(02)02044-2.

[47] A.P. Hammersley, S.O. Svensson, M. Hanfland, A.N. Fitch, D. Hausermann, Two-dimensional detector software: from real detector to idealised image or two-theta scan, High Pressure Res. 14 (1996) 235–248, https://doi.org/10.1080/08957959608201408.

[48] J.R. Lakowicz, F.G. Prendergast, D. Hogen, Differential polarized phase fluorometric investigations of diphenylhexatriene in lipid bilayers quantitation of hindered depolarizing rotations, Biochem. 18 (1979) 508–519, https://doi.org/10.1021/bi00570a02.

[49] J.R. Lakowicz, F.G. Prendergast, D. Hogen, Fluorescence anisotropy measurements under oxygen quenching conditions as a method to quantify the depolarizing rotations of fluorophores. Application to diphenylhexatriene in isotropic solvents and in lipid bilayers, Biochem. 18 (1979) 520–527, https://doi.org/10.1021/bi00570a022.

[50] M. Adler, T.R. Tritton, Fluorescence depolarization measurements on oriented membranes, Biophys. J. 53 (1988) 989–1005, https://doi.org/10.1016/S0006-3495(88)83179-5.

[51] N.C.S. Mykytczuk, J.T. Trevors, L.G. Leduc, G.D. Ferroni, Fluorescence polarization in studies of bacterial cytoplasmic membrane fluidity under environmental stress, Prog. Biophys. Mol. Biol. 95 (2007) 60–82, https://doi.org/10.1016/j.pbiomolbio.2007.05.001.

[52] T. Parasassi, G. De Stasio, A. d'Ubaldo, E. Gratton, Phase fluctuation in phospholipid membranes revealed by Laurdan fluorescence, Biophys. J. 57 (1990) 1179–1186, https://doi.org/10.1016/S0006-3495(90)82637-0.

[53] T. Parasassi, G. De Stasio, G. Ravagnan, R.M. Rusch, E. Gratton, Quantitation of lipid phases in phospholipid vesicles by the generalized polarization of Laurdan fluorescence, Biophys. J. 60 (1991) 179–189, https://doi.org/10.1016/S0006-3495(91)82041-0.

[54] T. Parasassi, E.K. Krasnowska, L. Bagatolli, E. Gratton, Laurdan and prodan as polarity-sensitive fluorescent membrane probes, J. Fluoresc. 8 (1998) 365–373, https://doi.org/10.1023/A:1020528716621.

[55] J.N. Weinstein, S. Yoshikami, P. Henkart, R. Blumenthal, W.A. Hagins, Liposome-cell interaction: transfer and intracellular release of a trapped fluorescent marker, Science 195 (1977) 489, https://doi.org/10.1126/science.835007.

[56] J. Barbet, P. Machy, A. Truneh, L.D. Leserman, Weak acid-induced release of liposome-encapsulated carboxyfluorescein, Biochim. Biophys. Acta 772 (1984) 347–356, https://doi.org/10.1016/0005-2736(84)90152-4.

[57] H. Matsuki, E. Miyazaki, F. Sakano, N. Tamai, S. Kaneshina, Thermotropic and barotropic phase transitions in bilayer membranes of ether-linked phospholipids with varying alkyl chain lengths, Biochim. Biophys. Acta 1768 (2007) 479–489, https://doi.org/10.1016/j.bbamem.2006.10.005.

[58] M. Yoshino, H. Takahashi, T. Takagi, T. Baba, K. Morita, H. Amii, T. Kanamori, M. Sonoyama, Effect of partial fluorination in the myristoyl groups on thermal and interfacial properties of dimyristoylphosphatidylcholine, Chem. Lett. 41 (2012) 1495–1497, https://doi.org/10.1246/cl.2012.1495.

[59] L.A. Bagatoll, T. Parasassi, G.D. Fidelio, E. Gratton, A Model for the interaction of 6-lauroyl-2-(N,N-dimethylamino)naphthalene with lipid environments: implications for spectral properties, Photochem. Photobiol. 70 (1999) 557–564, https://doi.org/10.1111/j.1751-1097.1999.tb08251.x.